

Conf-720331--2

The submitted manuscript has been authored by a contractor of the U. S. Government under contract No. W-31-109-ENG-38. Accordingly, the U. S. Government retains a nonexclusive, royalty-free license to publish or reproduce the published form of this contribution, or allow others to do so, for U. S. Government purposes.

ANL-HEP-CP--92-13

DE92 011197

ANL-HEP-CP-92-13

For the Proceedings of the Fourth Annual International Industrial Symposium on the Super Collider, March 4-6, 1992 New Orleans, Louisiana

MECHANICAL DESIGN AND FINITE ELEMENT ANALYSIS OF THE SDC CENTRAL CALORIMETER

V. Guarino,¹ N. F. Hill,¹ D. A. Hoecker,² T. D. Hordubay,²
J. Nasiatka,¹ D. W. Scherbarth,² R. L. Swensrud²

¹High Energy Physics Division
Argonne National Laboratory
9700 South Cass Avenue
Argonne, Illinois 60439

²Science and Technology Center
Westinghouse Electric Corporation
1310 Beulah Road
Pittsburgh, Pennsylvania 15235

Approved by OSTI
APR 01 1992

INTRODUCTION

When designing scintillating calorimeters for the study of particle interactions resulting from colliding beams, a primary goal is to instrument 100% of the available solid angle. In pursuit of this goal the challenge for mechanical designers is to minimize the amount of structural mass and still maintain acceptable engineering standards in the design.

Argonne National Laboratory, High Energy Physics involvement in the design of a central calorimeter for the SSC started in 1989. Our first proposal was to design a depleted uranium scintillator calorimeter similar to the ZEUS detector presently installed at the HERA electron-proton collider in Hamburg, Germany. Argonne was involved at the time in final assembly of modules for ZEUS that had been designed and constructed at ANL. Due to the cost of using depleted uranium, lead was chosen as the absorber material.

In collaboration with Westinghouse Science and Technology Center in Pittsburgh, Pennsylvania we embarked on a program to optimize the use of lead or lead alloys in the construction of the calorimeter. A cast lead design for the calorimeter evolved from this effort. Subsequent to this design, further pressure to reduce costs have now dictated a design which contains lead only in the electromagnetic sections of the calorimeter. The current design is shown in cross section in Fig. 1.

The finite element analysis we will present here was done using lead for the HAD1 section of the barrel.

CURRENT DESIGN

The current design calls for construction with the following base design features:

MASTER

DISCLAIMER

This report was prepared as an account of work sponsored by an agency of the United States Government. Neither the United States Government nor any agency thereof, nor any of their employees, makes any warranty, express or implied, or assumes any legal liability or responsibility for the accuracy, completeness, or usefulness of any information, apparatus, product, or process disclosed, or represents that its use would not infringe privately owned rights. Reference herein to any specific commercial product, process, or service by trade name, trademark, manufacturer, or otherwise does not necessarily constitute or imply its endorsement, recommendation, or favoring by the United States Government or any agency thereof. The views and opinions of authors expressed herein do not necessarily state or reflect those of the United States Government or any agency thereof.

Tile/Fiber Projective Calorimeter
 Model-G
 (Quadrant Cross Section)

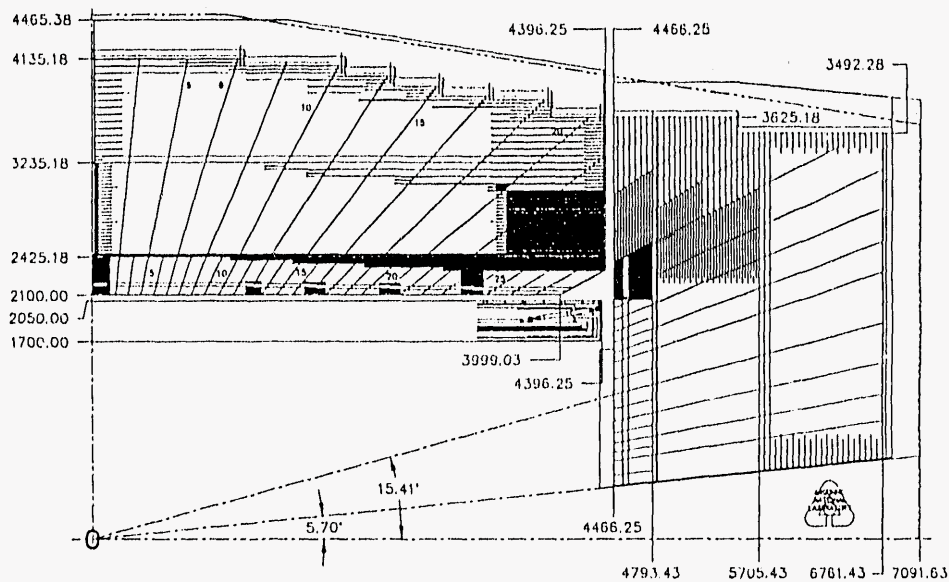


Figure 1. Cross section of one quadrant of the barrel calorimeter.

Barrel Calorimeter (Fig. 2):

Size: \approx 9 meters in diameter \times 9 meters in length

Weight: 1/2 barrel = 1376 tons
 1/32 wedge = 43 tons

Segmentation: 32 wedges made up of 64 symmetric module pairs

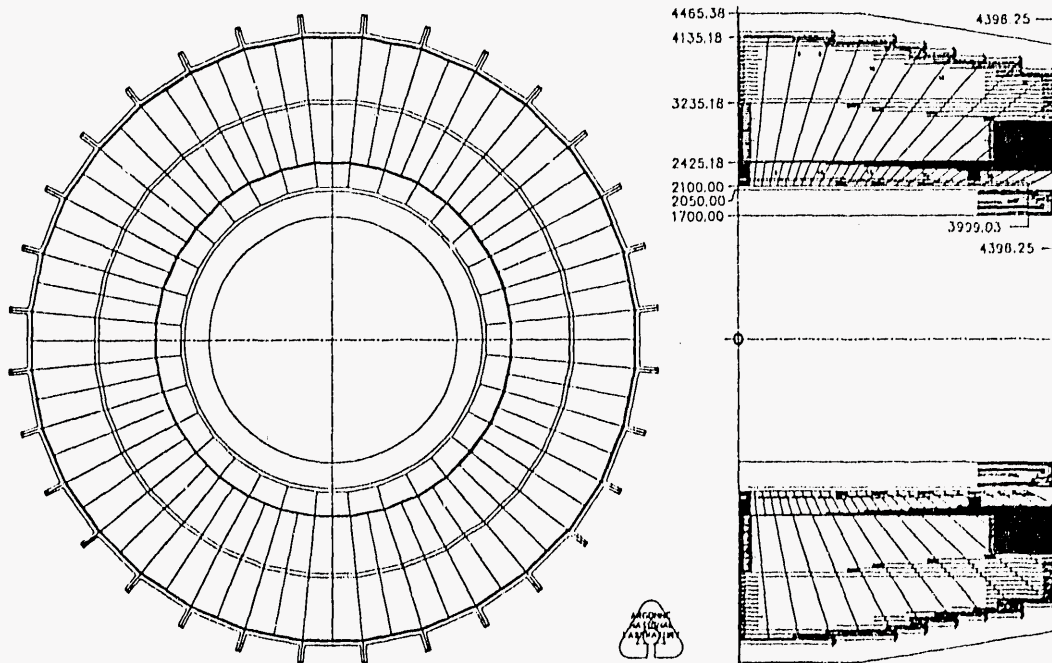


Figure 2. Cross section of 1/2 of the barrel calorimeter.

End Cap Calorimeter (Fig. 3):

Size: \approx 8 meters in diameter \times 2.5 meters in length

Weight: each end cap = 680 tons
1/32 wedge = 21.25 tons

Segmentation: 32 wedges

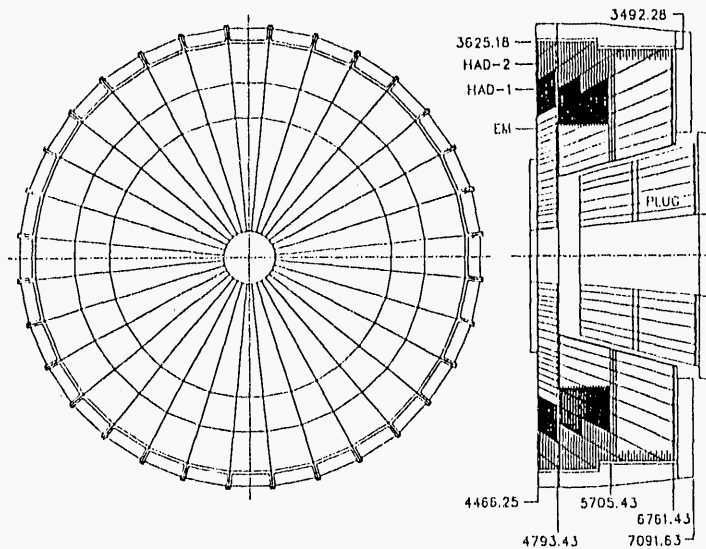


Figure 3. Cross section of the end cap calorimeter.

The barrel calorimeter is constructed using 9 mm (.354 in) steel plates in HAD1 and 24 mm (.945 in) steel plates in HAD2 joined together by welded spacer plates that are alternated to form pockets for the plastic scintillator tiles. This arrangement is shown in Fig. 4.

The readout of the scintillator tiles is achieved by embedded optical fibers that are routed to photomultiplier tubes at the outer radius of the detector.

The construction of the end cap calorimeter is similar except that the absorber plates are arrayed perpendicular to the detector longitudinal axis.

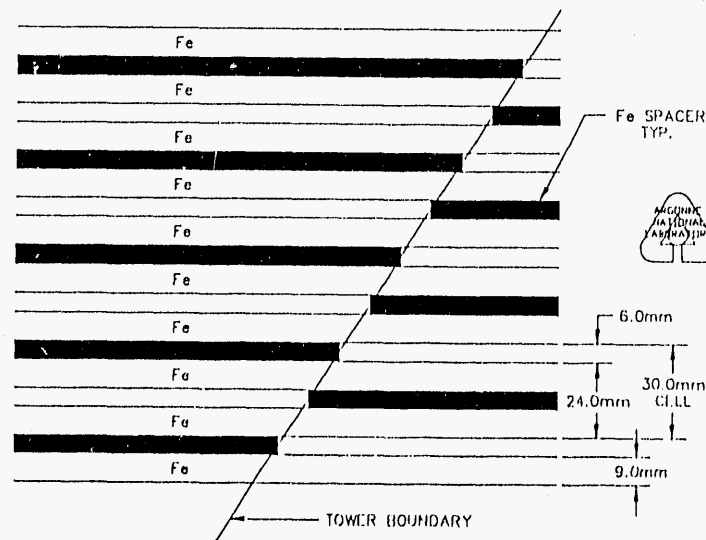


Figure 4. HAD1/HAD2 internal structure.

FINITE ELEMENT ANALYSIS

Differences between Model and Current Design

The finite element analysis was done on the configuration shown however, the HAD1 sections of the barrel were constructed using cast lead as the absorber. A recent change in design has dictated that these segments of the detector now be fabricated with steel plates. The data for the barrel calorimeter presented here represents the lead design. The primary changes in the data, that will be realized with this change, are a reduction in overall weight and an increase in the stiffness of the system. The analysis is presently being re-run using steel for these segments. The electromagnetic section of both the barrel and the end cap are still designed for cast lead.

Model Construction

All of the analysis referred to in this paper was done using Cosmos M a product of the Structural Research Analysis Corporation, Santa Monica, California. Due to size limitations within Cosmos, it was not possible to mesh the 3D model with all of the details of actual construction. In order to deal with this limitation, it was decided to use individual wedges that were somewhat less detailed to construct the assembly. The interface forces and deflections were then calculated and the results will be applied to a fine meshed model of the individual wedge. The simplified model used the following method for construction. The structural frame which consists of the inner and outer plates, the end plates, and the connecting bulkhead membranes were modeled in detail. The lead absorber plates, due to the complexity of modeling laminate structures, were represented as solids with the stiffness and density modified to represent the lead plate construction. The composite stiffness used to model the lead structure was determined by using the ratio of load carrying area to the total area and using this ratio to modify the stiffness of solid lead. The densities are represented by using the ratio of total volume to occupied volume.

In connecting the wedge model into the assembly, the interface boundaries between modules were separated by .030" and connected at discreet points along those boundaries. The location of these points is shown in Fig. 5. These points were deliberately chosen since they represent actual boundary load transfer points. The difference between modeled nodes and actual nodes was in the quantity. The design construction will increase the number of load transfer points by a factor of five in most cases.

○ DENOTES CONNECTING POINTS

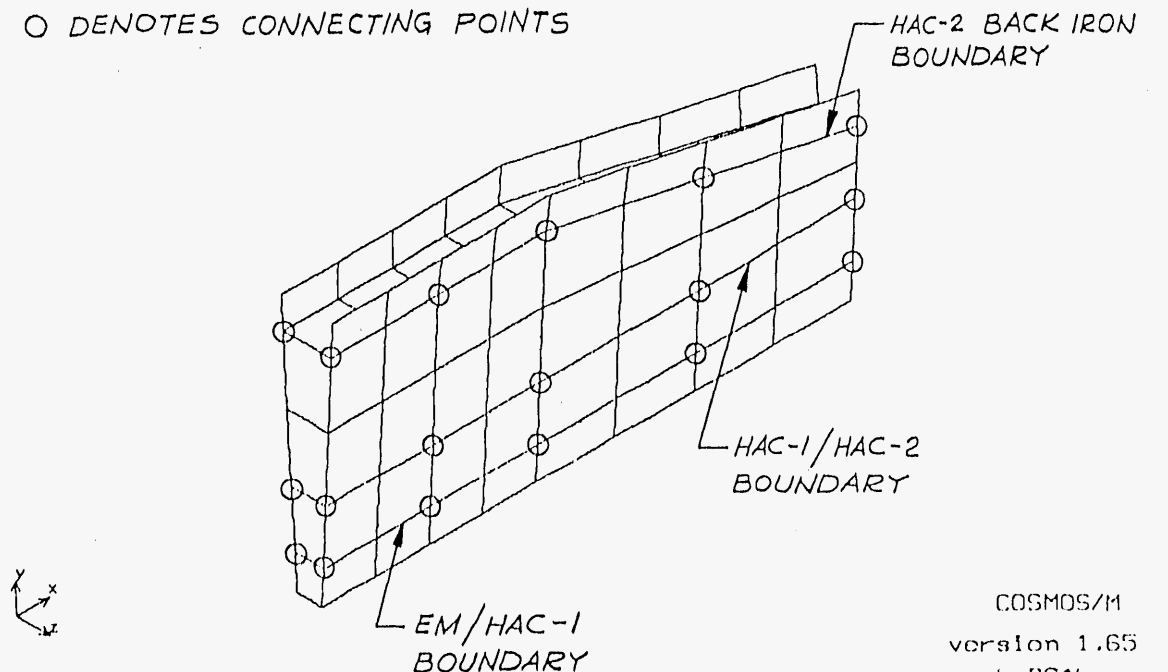


Figure 5. Wedge module connecting points.

The final assembled quarter barrel is represented in Fig. 6.

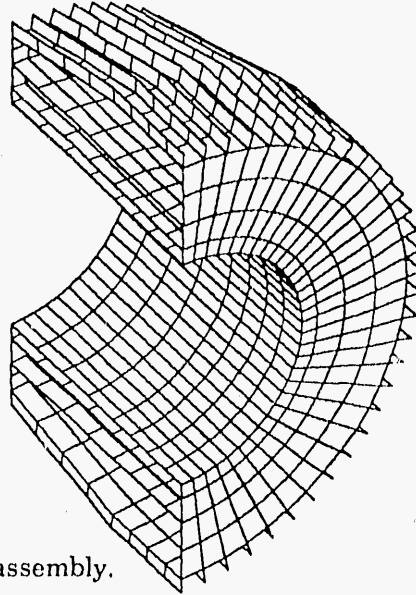


Figure 6. Quarter barrel assembly.

Analysis Results for the Barrel Calorimeter

The EM, HAD1 and HAD2 sections are layered structures that have been approximated by solid elements. Since the stiffness of these sections is unknown, certain assumptions were made. The HAD2 section is a welded structure with alternating cells, therefore it was felt that the modulus of steel, 60×10^6 psi, would be a good approximation of the HAD2 stiffness. The HAD1 and EM sections however are composed of layers of lead connected together with thin (.020 in.) bulkheads. The stiffness of these structures obviously is much lower than that of solid lead. In order to establish limits for this situation, it was reasoned that by setting upper and lower boundary conditions, the extreme limits of the problem would be established. The upper limit of the stiffness of these sections is the modulus of solid lead, the lower limit was found by taking the ratio of the load carrying area to the area of a cell (the bulkhead area) to the total area of a cell and multiplying it by the modulus of lead. Separate cases of the analysis were then run using these upper and lower limits of the EM and HAC1 stiffness. This method will not allow exact values of the connecting forces to be calculated, however we will be able to maximize these forces and design for the maximum condition.

Four different cases were run using a combination of stiffnesses for the EM and HAD1 sections and using different size rods to connect the modules together. The cases are summarized in Table 1. The use of different size rods allowed us to study the effect of size on the connections. As one will see later this had little effect.

Table 1. Case numbers for Connection and stiffness variations.

Case #	EM Stiffness (psi)	HAD1 Stiffness (psi)	Rod. Diameter (inch)
1 (Lead Modulus)	2×10^6	2×10^6	1/4
2 (Modified Modulus)	24×10^3	35×10^3	1/4
3 (Lead Modulus)	2×10^6	2×10^6	1
4 (Modified Modulus)	24×10^3	35×10^3	1

The connecting forces calculated for the barrel are forces which are distributed along the length of the boundary plates. For example if a maximum normal connecting force of 400,000 lbs. is found along the EM-HAD1 boundary, and this boundary has 29 bearing points at which the modules are connected, and each point has a cross sectional area of 1

square inch, then each point carries a load of $\approx 14,000$ lbs. and has a stress of 14,000 psi. The summation of the forces, both normal to the interface surfaces and the radial and axial shear loads are represented in Figs. 7 through 9.

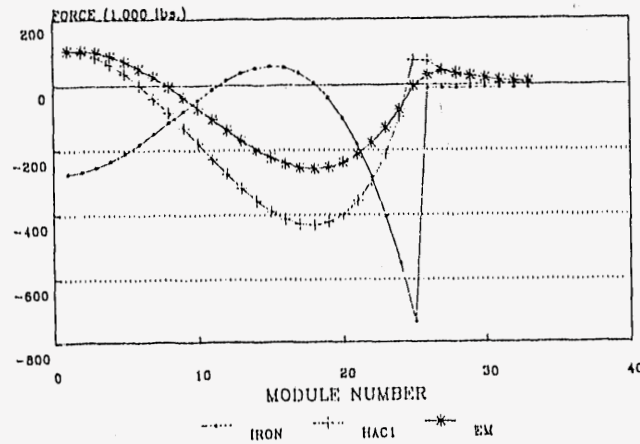


Figure 7. Forces normal to the surface as a function of module position.

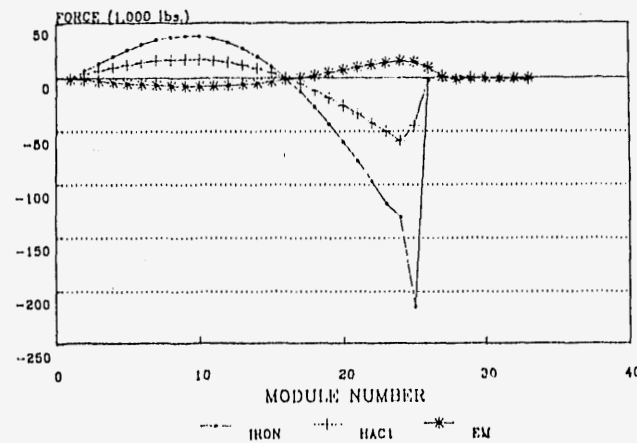


Figure 8. Radial shear force as a function of module position.

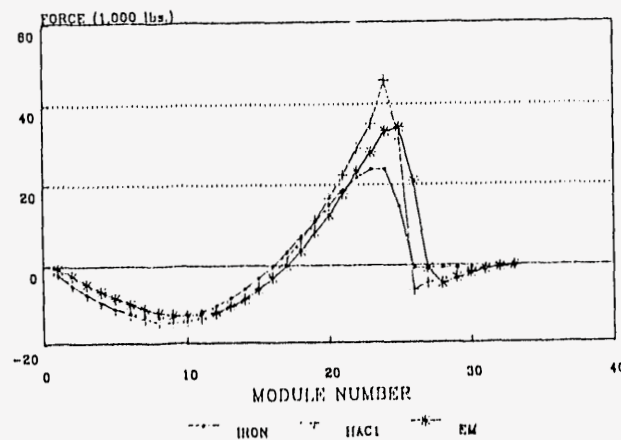


Figure 9. Beam direction shear forces as a function of module position.

When the lead in the HAD1 section is replaced with steel the forces indicated will be reduced by the decrease in weight, however the individual connecting forces will change due to the increased stiffness.

Endcap Calorimeter Model

The endcap was modeled in a manner similar to that of the barrel. The EM front plate, the EM-HAD1 boundary plate, HAD1-HAD2 boundary plate and the back iron structure were modeled first using plate elements with the appropriate thicknesses to form the basic frame as shown in Fig. 10. The individual modules were connected to each other at 22 points, 8 along the EM-HAD1 boundary, 6 along the HAD1-HAD2 boundary and 8 along the back iron. The EM section once again is composed of layers of lead plates separated by thin bulkheads. This presents the same problem of modeling as it did in the barrel, how to model the stiffness of these structures appropriately. Instead of modeling the EM and HAD1 structures using solid elements and then varying the stiffnesses of this solid to approximate the stiffness of the structures, individual plates of lead were used. The EM section has 12 lead plates 10.5 mm thick separated by bulkheads, these were approximated by 4 plates which were 1.24" thick and separated by 7 bulkheads. This method approximates the stiffness of the EM structure but does not go into so much detail that the problem becomes too large to run. Similarly the HAD1 section has 28 steel plates 20.5 mm thick which were approximated by 5 plates which were 4.5" thick and separated by 9 bulkheads. The stiffness of lead, 2×10^6 psi, was used for all of these plates. The HAD2 section was approximated by solid elements and the stiffness of steel, 30×10^6 psi, was used since HAD2 is a welded structure with very few cells therefore it was felt that it would behave like a solid structure. Figure 11 shows the module wedge and the position of the connecting points. This module was then copied and rotated to form a half endcap as shown in Fig. 12. Advantage was taken of symmetry so that only half of the endcap was modeled which reduced the size of the problem and computer time considerably. The bottom 4 modules were fully supported along the entire length of the outside diameter of the structural iron.

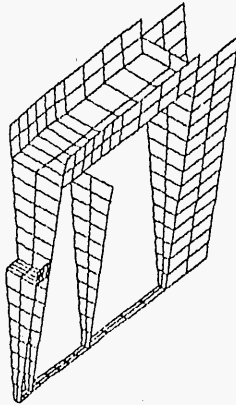


Figure 10. Wedge module frame rough model.

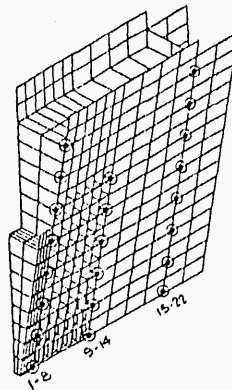


Figure 11. Wedge connecting points.

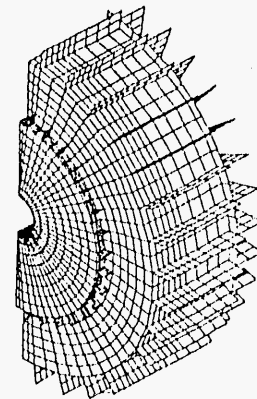


Figure 12. One half end cap assembly.

Analysis Results for the End Cap Calorimeter

The results of this analysis produced similar results to those obtained for the barrel. Three representative plots of the results are shown as Figs. 13, 14, 15. A summary of the maximum forces expected at any interface boundary are represented in Table 2.

Table 2. Interface boundary maximum forces.

Boundary	Max. Normal Force	Max. Radial Shear	Max. Z Dir. Shear
EM/HAD 1	+0 (tension) -17,000 lbs. (compr)	-3,000 (inward) +7,000 (outward)	-2000 +2000
HAD1/HAD 2	+0 -30,000	-10,000 +12,000	+2,000 +2,000
Outer Row	+2,000 -35,000	-15,000 +15,000	+12,000 +2,000

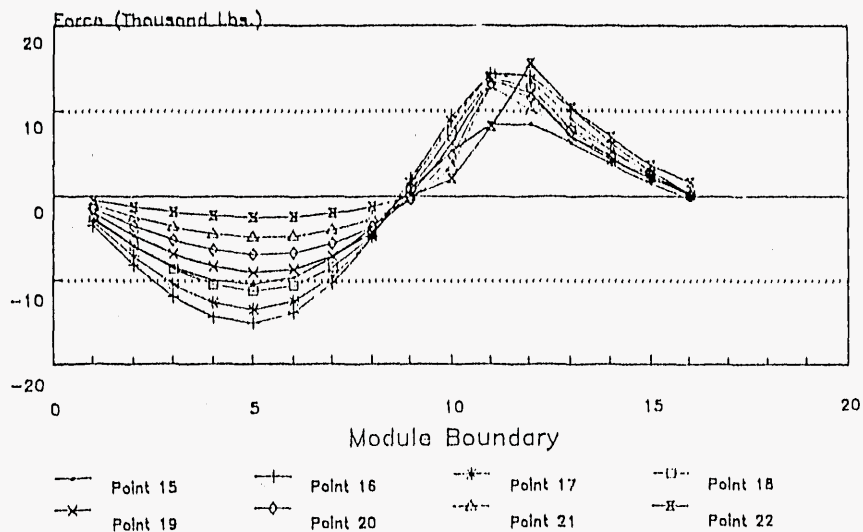


Figure 13. Outer iron normal forces.

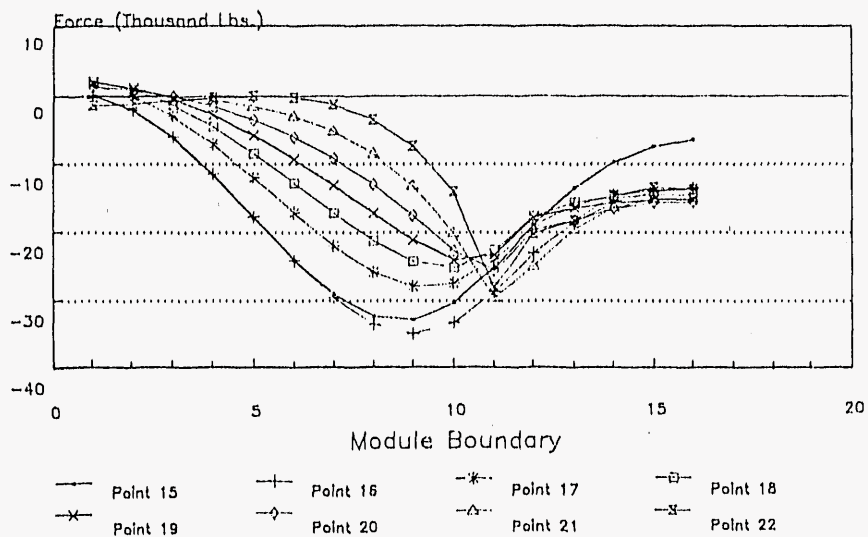


Figure 14. Outer iron radial shear forces.

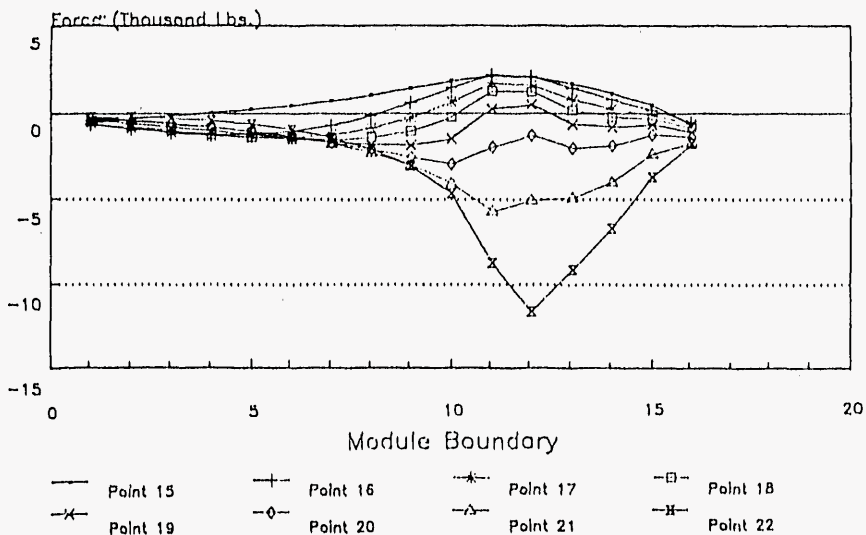


Figure 15. Outer iron Z direction forces.

* Work supported in part by the U.S. Department of Energy, Division of High Energy Physics, Contract W-31-109-ENG-38.

END

**DATE
FILMED
6/01/92**

